Quantum oscillations in the heat capacity of Kondo insulator YbB_{12}

Kuan-Wen Chen[1†], Yuan Zhu[1†], Danilo Ratkovski[2], Guoxin Zheng[1], Dechen Zhang[1], Aaron Chan[1], Kaila Jenkins[1], Joanna Blawat[3], Tomoya Asaba[4], Fumitoshi Iga[5], Chandra M. Varma[6], Yuji Matsuda[4,7], John Singleton[3], Alimamy F. Bangura[2], and Lu Li[1*]

[1] *Department of Physics, University of Michigan, Ann Arbor, MI 48109, USA*
[2] *National High Magnetic Field Laboratory, 1800 East Paul Dirac Drive, Tallahassee, Florida 32310-3706, USA*
[3] *National High Magnetic Field Laboratory, MS E536, Los Alamos National Laboratory, Los Alamos, NM 87545, USA*
[4] *Department of Physics, Kyoto University, Kyoto 606-8502, Japan*
[5] *Institute of Quantum Beam Science, Graduate School of Science and Engineering, Ibaraki University, Mito 310-8512, Japan*
[6] *Department of Physics, University of California, Riverside, CA. 92521*
[7] *Los Alamos National Laboratory, Los Alamos, New Mexico 87545, USA*

(Dated: September 10, 2025)

We observe magnetic quantum oscillations in the heat capacity of the Kondo insulator YbB_{12}. The frequency of these oscillations, $F = 700$ T, agrees with that from magnetoresistance and torque magnetometry experiments for $\mu_0 H > 35$ T in the Kondo insulating phase. Remarkably, the quantum-oscillation amplitudes in the heat capacity are substantial, with $\Delta\tilde{C}/T \approx 0.5$ mJ mol^{-1}K^{-2} at 0.8 K, accounting for 13% of the known linear heat capacity coefficient γ. Double-peak structures of quantum-oscillation amplitudes due to the distribution function of fermions were identified and used to determine the value of the effective mass from the heat capacity, which agrees well with that from torque magnetometry. These observations support bulk charge-neutral fermions contributing to the quantum oscillations in YbB_{12}.

PACS numbers:

Quantum oscillations have traditionally served as a direct probe of the Fermi surfaces of metals [1]. Surprisingly, in recent years, these oscillations have also been observed in electrical insulators, where a Fermi surface was previously thought to be absent, challenging our understanding of electronic band structure. This phenomenon has been detected in insulating phases such as Kondo insulators (e.g. SmB_6 [2, 3], YbB_{12} [4–8]), insulating InAs/GaSb quantum wells [9, 10], and the kagome Mott insulator $YCu_3(OH)_6Br_2[Br_x(OH)_{1-x}]$ [11, 12].

In the Kondo insulator YbB_{12}, quantum oscillations were measured by several groups independently [4, 5, 7]. The oscillations are observed in both resistivity ρ (the Shubnikov-de Haas (SdH) effect) and magnetization M (the de Haas-van Alphen(dHvA) effect). The oscillations are periodic in $1/B$, and their T-dependence follows the Lifshitz-Kosevich (LK) formula [8].

Additionally, a finite linear heat capacity coefficient γ, approximately 3.8 mJmol^{-1}K^{-2}, was observed in heat-capacity measurements [6]. This value agrees with the Fermi surface size and effective mass deduced from quantum oscillations, suggesting that the latter represents a bulk (rather than surface) phenomenon. A finite residual T-linear term in the thermal conductivity is also observed $\kappa_{xx}/T \neq 0$ ($T \to 0$), indicating itinerant and gapless excitations [6]. Furthermore, a recent study observed double peak features in heat capacity of YbB_{12} in applied magnetic field, providing evidence for fermionic excitations [13]. However, the upper field limit was 35 T, below where quantum oscillations with $1/B$ periodicity were confirmed in magnetization and electrical resistivity [4, 5, 7]. Various theoretical models have been proposed to explain types of quasiparticles that can transport heat and respond to magnetic vector potential through quantum oscillations, yet do not transport charge [14–27].

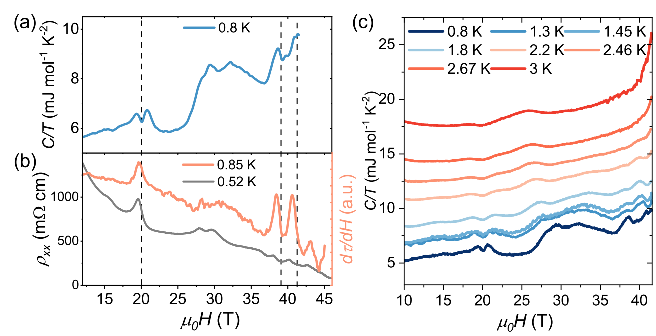

FIG. 1: (a) Heat capacity divided by temperature C/T as a function of the magnetic field at 0.8 K displays a distinctive double-peak structure at a transition at $\mu_0 H \approx 20$ T and quantum oscillations above 35 T. (b) Resistivity ρ_{xx} and the field derivative of torque $d\tau/dH$ as function of the magnetic field at 0.52 K and 0.85 K, respectively. Dashed lines mark the location of the transition at around 20 T and quantum oscillations above 35 T. (c) C/T as a function of the magnetic field at various temperatures.

However, the community has not yet reached a consensus on fundamental questions about the quantum oscillations; debates persist about whether the oscillations originate from the surface or the bulk and whether they are intrinsic or extrinsic. It is essential to obtain direct *thermodynamic* evidence to determine whether the above-mentioned thermal properties originate from the same quasiparticle band as the quantum oscillations.

In this work, we report quantum oscillations in the heat capacity of YbB_{12} above 35 T. The quantum oscillations observed in heat capacity are in good agreement with previous reports of SdH and dHvA oscillations [8, 28], with consistent effective masses obtained. The large amplitude of the oscillations, reaching 13% of the background heat capacity, strongly supports an intrinsic bulk origin and the neutral fermion picture of the oscillations in YbB_{12}. The square-root dependence of high-field magnetization and the absence of spin-splitting in the insulating state in the heat capacity oscillations provide further support for the spin- and charge-neutral fermion theory proposed in [14, 15].

Figure 1(a) presents the variation of the heat capacity divided by temperature, C/T, in magnetic fields of up to 41 T obtained using a DC field magnet. The heat-capacity findings align closely with previous magnetoresistance (MR) and torque measurements, as reported in [4] (see Fig. 1(b)). Quantum oscillations with a frequency $F = 700$ T are detected in C/T, magnetoresistance (ρ_{xx}), and torque (τ) measurements for $\mu_0 H > 35$ T. An electronic transition is identified near magnetic field $\mu_0 H_0 = 20$ T [8]. Moreover, a distinctive double-peak structure associated with both the $\mu_0 H_0 = 20$ T transition and quantum oscillations is evident in the heat capacity data.

The transition at $\mu_0 H_0 = 20$ T was originally associated with a Lifshitz transition of the electronic structure [8] in which the Fermi surface(s) of charge-neutral quasiparticles undergo transitions driven by the Zeeman energy, leading to features in the magnetic torque [8], and (here) the heat capacity. At the same time, residual charged electrons and/or holes scatter from the charge-neutral FS, producing corresponding signatures in the magnetoresistance [8]. Thermopower also displays features at the same magnetic field, $\mu_0 H_0 = 20$ T, as will be shown later. However, our direct measurements of the heat capacity reveal that its value very similar on either side of the transition. Moreover, the Hall conductivity measurement does not show any significant change in carrier density [8]. Finally, the earlier measurements of the heat capacity at lower fields show values of the fermionic γ-term that are consistent with a simple spherical model of the Fermi surface based on the dHvA oscillations above 35 T [6]. All of these observations suggest that, in case of YbB_{12}, the density of states hardly changes across this $\mu_0 H_0 = 20$ T transition. In this context, we note that the Fermi Surface of copper is a large sphere with some small connecting necks; its electronic heat capacity is dominated by the spherical part of the FS. In an analogous fashion, perhaps only some small neck orbits (dis)appear at the 20 T transition in YbB_{12}. As this transition provides the dominant feature in the heat capacity for $H > H_0$, to be consistent with previous literature, we refer to it as a Lifshitz transition.

The detection of a double-peak structure in the heat capacity at Lifshitz transitions has been observed in heavy-fermion compounds such as $CeRu_2Si_2$ [31] and UCoGe [43]. The existence of double-peak structures in the quantum oscillations of heat capacity has been theoretically predicted [32] and, more recently, experimentally identified in natural graphite, with a comprehensive analysis provided by Yang et al. [43]. For fermionic quasiparticles, the relationship between heat capacity over temperature and the quasiparticle energy spectrum is given by

$$\frac{C}{T} = k_B^2 \int_{-\infty}^{\infty} D(E) \left(- \left(\frac{E - E_F}{k_B T} \right)^2 \frac{\partial f}{\partial E} \right) \mathrm{d}E, \qquad (1)$$

where f is Fermi-Dirac distribution function $f = 1/(e^{(E-E_F)/k_B T} + 1)$ and $D(E)$ is the density of states. Unlike the kernel term $-\mathrm{d}f/\mathrm{d}E$ in electrical conductivity, the dual-peak structure originates from the kernel term $-(E - E_F)^2 \mathrm{d}f/\mathrm{d}E$ in heat capacity. Moreover, the quasiparticles probed are distributed around the chemical potential at finite temperatures, which is temperature-dependent. The separation between the resulting maxima increases linearly with temperature as $\Delta E = 4.8\ k_B T$ and disappears at zero temperature (see Supplement Material [44] Fig. S3(a)). The behavior of C/T versus $\mu_0 H$ at various temperatures, depicted in Fig. 1(c), comes from measurements on the same sample in the NHMFL 35 T and 41 T magnets. At higher temperatures, specifically for $T > 2.67$ K, the dramatic increase in C/T for $\mu_0 H > 40$ T is associated with a metal-insulator transition. The quantum oscillation amplitudes at 0.8 K are substantial, with $\Delta\tilde{C}/T \approx 0.5$ mJmol^{-1}K^{-2}, accounting for 13% of the known linear heat capacity coefficient $\gamma \approx 3.8$ mJmol^{-1}K^{-2} [6]. Thus, it is plausible that the same neutral quasiparticles contribute to both the quantum oscillations and the γ coefficient, allowing us to rule out the hypothesis that quantum oscillations arise from impurity phases or from surface contributions [20, 25].

The temperature dependence of the 20 T Lifshitz transition in the heat capacity of YbB_{12} as well as signatures in the Seebeck coefficient are plotted in Fig. S2, and a detailed discussion is included in Supplementary Materials Section B. To summarize, the temperature evolution of the double peak structure can be modeled well using a single symmetric DOS convoluting with the kernel term $-(E - E_F)^2 \mathrm{d}f/\mathrm{d}E$ in Eqn. 1. The energy separation $\mathrm{d}E/\mathrm{d}(\mu_0 H) = 0.265$ meV/T obtained from the Lifshitz transition is consistent with a recent report on heat capacity in YbB_{12} by Yang et al., whose $\mathrm{d}E/d(\mu_0 H) = 0.258$ meV/T [13]. We also note a series of peak structures in heat capacity around 30 T, and their nature is discussed in the Supplementary Materi-

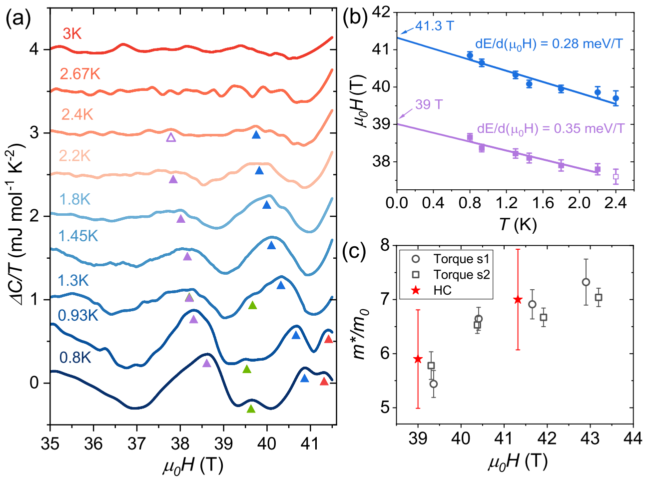

FIG. 2: (a) The oscillatory component of the heat capacity divided by temperature $\Delta C/T$ at various temperatures after subtracting the polynomial backgrounds. The curves are shifted vertically for clarity. The triangles mark the peak positions. The 2.4 K peak near $\mu_0 H = 38$ T is marked by an empty triangle due to uncertainty in determining its position. (b) Magnetic field positions of the dominant peaks as a function of temperature. The lines are linear fits of the data. The error bars show the uncertainty of defining the peak positions. Excluding or including the 2.4 K purple point does not affect the fitting result. (c) Field dependence of the effective masses $m^*(39\text{ T}) = 5.9\ \text{m}_0$ and $m^*(41.3\text{ T}) = 7\ \text{m}_0$ from heat capacity compared to the effective masses obtained from the LK fits to the dHvA oscillation amplitudes in torque [4], where m_0 is the free electron mass.

als section C and Fig. S4. We will mainly focus on the discussion of the heat capacity quantum oscillations appearing above 35 T in the following text.

In Fig. 2(a), $\Delta C/T$ exhibits the $F = 700$ T quantum oscillations also seen in resistivity and torque once a polynomial background is subtracted. Two double-peak structures can be clearly observed. Unlike the Lifshitz transition, the double-peak structure in quantum oscillations is asymmetric. The peak at a lower magnetic field is more prominent, while the peak at a higher magnetic field is less intense. This asymmetry is attributed to the asymmetric density of states $D(E)$ in the 3D Landau levels of quasiparticles in YbB_{12}. As shown in Supplementary Material Fig. S5, it is well known that the energy of band electrons is quantized into Landau levels in the plane perpendicular to the magnetic field. The "sawtooth" structure in the density of states results from the one-dimensional motion parallel to $\mathbf{H}$ (DOS $\propto 1/\sqrt{E}$) superimposed on the δ-function-like Landau levels. Similar considerations are expected to apply to the neutral fermions producing the quantum oscillations in YbB_{12} [8, 14, 15]. In Fig. 2(b), we plot the location of the dominant low-field peak versus temperature. The linear intercepts give the zero-temperature positions of the two double peak structures to be $\mu_0 H = 39$ T and $\mu_0 H = 41.3$ T. This gives a quantum-oscillation frequency of 700 T, and corresponding Landau indices $n = 18$ and $n = 17$. The 1/B periodicity of the oscillations is confirmed in Supplementary material Fig. S6. Unfortunately, the thermopower data of YbB_{12} were only measured up to 31 T. At higher magnetic fields, we expect the thermopower to exhibit quantum oscillations in the form of asymmetric double peaks, as shown in the simulation in Fig. S3 (e).

Fermions obey the Fermi-Dirac distribution. Therefore, the smearing of quantum oscillation amplitude due to increasing temperature follows a specific form given by Lifshitz-Kosevich (LK) theory. Thermodynamic quantities such as magnetization and heat capacity arise from oscillations in the thermodynamic potential $\tilde{\Omega} = \tilde{\Omega}_0 R_T(T)$, where $\tilde{\Omega}_0$ is the zero temperature potential. The damping factor $R_T = z/\sinh(z)$ is a direct consequence of the smearing of the Fermi–Dirac distribution function near the Fermi energy, where $z = 2\pi^2 p k_B m^* T/e\hbar B$, m^* is the effective mass, m_e is the free electron mass, and p is an integer denoting the harmonic. Consequently, the oscillations in magnetization, $\tilde{M} = -\frac{\partial\tilde{\Omega}}{\partial B}$, are proportional to R_T. The F=700 T quantum oscillation in torque $\Delta\tau$ and magnetoresistivity $\Delta\rho_{xx}$ has been shown to be well described by the R_T in the LK formula by Xiang et al. [4, 8], consistent with Fermionic quasiparticles. Regarding the heat capacity, $\Delta\tilde{C}/T = -\frac{\partial}{\partial T}\left(\frac{\partial\tilde{\Omega}}{\partial T}\right)$, the damping factor is defined as $R''_T(z) = z(\left(\frac{2\cosh(z)}{\sinh^2(z)}\right) - z(1 + \frac{\cosh^2(z)}{\sinh^3(z)}))$ [35, 36]. $\Delta\tilde{C}/T$ changes sign and exhibits a "π-phase shift" at $z = 1.6$ where $R''_T(z = 1.6) = 0$ (Supplemental Material Fig. S7). This point is commonly used to determine the effective mass m^* [37, 38]. However, such a "π-phase shift" is not discernible in the double-peak structure. The experimental observation of a single- or double-peak structure depends on the measured range of temperatures, the effective mass, and the Landau level width. Here, we introduce a method to determine the effective mass via the double-peak structure of the heat capacity. Since the peak at the higher magnetic field in a double-peak structure is identifiable only at temperatures below $T = 1.3$ K for both Landau levels ($n = 18$ and $n = 17$), we plot only the positions of the dominant lower field peaks against temperature in Fig. 2(b), revealing a linear relationship. $\Delta E = \Delta(\mu_0 H)\cdot \mathrm{d}E/\mathrm{d}(\mu_0 H) \approx 2.4\ k_B T$ should be satisfied, as shown in Supplemental Material Fig. S3(a), where ΔE is the shift of the dominant lower field peak from zero temperature. By fitting the slope in Fig. 3(b), $\mathrm{d}E/\mathrm{d}(\mu_0 H) = 0.35$ meV/T for $n = 18$ and 0.28 meV/T for $n = 17$ were deduced. From the Landau-level energy $E = n\hbar\omega_c$, where $\omega_c = eB/m^*$, we are able to obtain the effective masses $m^*(n = 18) = 5.9\ m_0$ and $m^*(n = 17) = 7\ m_0$. These results are in good agreement with the previous dHvA torque data, as shown in

Fig. 2(c).

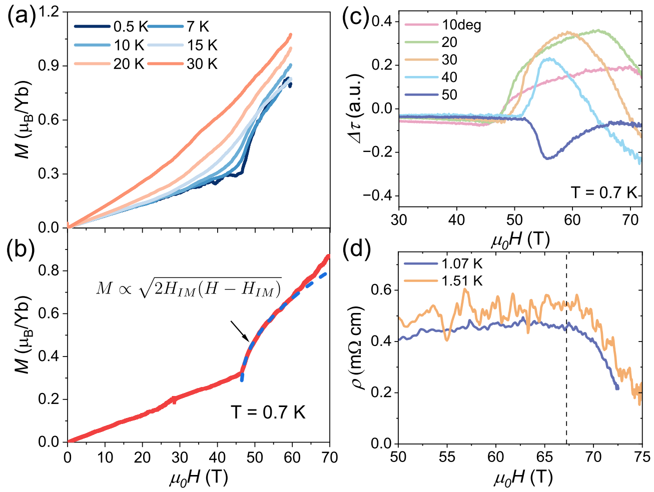

FIG. 3: (a) Magnetization measurement at various temperatures using a compensated-coil extraction magnetometer in a 60 T pulsed magnet. The field is applied along the [100] direction. (b) Magnetization measurement at 0.7 K in the 75 T Duplex magnet. The fitted curve, depicted in blue, represents $\sqrt{2H_{\mathrm{IM}}(H-H_{\mathrm{IM}})}$ where H_{IM} =46.5 T is the I-M transition field. (c) Torque $\Delta\tau$ with a linear background subtracted at various angles from H ∥ [100] (0 degrees) to H ∥ [001] (90 degrees). (d) Magneto-resistivity measurement in the 75 T Duplex magnet [28]. A downward kink is observed at 67 T.

An insulator-to-metal (I-M) transition at fields between $\mu_0 H_{\mathrm{IM}} \approx 45-47$ T at low temperatures is shown in Fig. 3(a) and has been reported in literature [28, 39, 42]. The quantum oscillations in the field-induced metallic state in YbB_{12} have been observed independently by groups using proximity detector oscillator (PDO) [28, 30], and tunnel-diode oscillator (TDO) techniques [7]. It has been suggested that the same quasiparticle band gives rise to the quantum oscillations in both insulating and metallic states. Note that we neglected the Zeeman energy (i.e. $E_Z = g_J m_J \mu_{\mathrm{B}} H = 0$) in $\mathrm{d}E/\mathrm{d}H$ in heat capacity for the insulating state and derived effective masses consistent with those deduced from torque measurements using the LK formula. Furthermore, spin-splitting of Landau level is not observed in heat capacity in the insulating state, which agrees with previous quantum-oscillation observations in torque τ and resistivity ρ_{xx} indicating the absence of spin-splitting effects in the Kondo insulating state. This is a property of spin-less (as well as charge-less) fermions predicted in refs. [14, 15]. In contrast, spin-splitting emerges in the Kondo metallic state, characterized by a g-factor of 0.084 [28]. In this Kondo metallic state, neutral particles start to decay into electrons and holes once the field exceeds $\mu_0 H_{\mathrm{IM}}$. This process is accompanied by the appearance of Zeeman splitting, which contributes to the magnetization. This contribution can be expressed as magnetization $M \propto \sqrt{2H_{\mathrm{IM}}(H-H_{\mathrm{IM}})}$ in ref [15]. In Fig. 3(b), a sharp increase of the magnetization shows up right after the I-M transition. Beyond 65 T, the magnetization deviates from the $\sqrt{2H_{\mathrm{IM}}(H-H_{\mathrm{IM}})}$ and has a paramagnetic linear behavior instead. A more pronounced feature is shown in the torque measurements, which are also sensitive to the anisotropy of magnetic susceptibility. As shown in Fig. 3(c), there is a significant increase in torque at the I-M transition and a subsequent decrease at the higher field (65 - 70 T for angles close to H ∥ [100]). The magnitude of M does not exhibit a sharp change, indicating that the total density of states in YbB_{12} does not undergo a dramatic change. The linear field dependence of M and the notable decrease in $\Delta\tau$ imply that M rotates and tends to align with the direction of the magnetic field. According to the two-fluid scenario in ref. [8], in the Kondo metal state, fermions scatter between charge-neutral Landau levels and heavy-fermion metal bands, leading to the SdH effect in ρ_{xx}. The emergence of the new state at around 70-75 T implies the possible end of the neutral fermions, where the elimination of the density of states (DOS) for these fermions leads to reduced scattering of more conventional heavy electrons, thereby leading to a decrease in ρ_{xx} as shown in Fig. 3(d).

Quantum oscillations in the heat capacity, together with previous studies [4, 8, 28], provide insight into modeling the observations in the Kondo insulator YbB_{12}. The observation of the Lifshitz transition suggests that under a 20 T magnetic field, the bulk ground state of the mixed valence insulator YbB_{12} may shift to a new state with a mixture of charge-neutral fermions and a small charge gap. When the magnetic field exceeds 35 T, it becomes strong enough to reveal Landau level quantization in the thermodynamics of these charge-neutral fermions. This Landau-level quantization permeates the bulk of YbB_{12}, showing up most clearly in heat capacity and torque oscillations and, via some scattering mechanisms with charged carriers, also in its residual resistivity. This state persists until a stronger field is sufficient to close the charge gap. This charge-neutral fermion picture explains the quantum oscillations observed in torque, resistivity, and heat capacity in the insulating state, if coupled with a possible scattering mechanism such as the one proposed in Ref. [8]. Our results motivate further experiments in YbB_{12}, including searches for quantum oscillations in thermoelectric effects and for cyclotron resonance in the 35–45 T field range.

In conclusion, quantum oscillations are observed in the heat capacity in insulating YbB_{12}. The frequency $F = 700$ T can be derived from the inverse magnetic field of the double peak centers. The effective masses are derived using a method based on the linear relation between double-peak separation and temperature, and are consistent with those deduced from the magnetoresistance and torque via the LK formula. The large quantum oscillation amplitude (13 % of the known linear heat capacity coefficient γ) is evidence for an intrinsic bulk signal, strongly supporting itinerant, charge-neutral excitations in YbB_{12}. The Liftshiz transition around $B = 20$ T is confirmed by heat-capacity and thermopower measurements. In the extreme magnetic field beyond $\mu_0 H = 65$ T, the magnetization M deviates from the $\sqrt{2H_{\mathrm{IM}}(H - H_{\mathrm{IM}})}$ dependence and has a paramagnetic linear behavior; a pronounced feature is also shown in torque and resistivity, indicating the emergence of a new state where the magnetization M rotates and tends to align with the direction of the applied magnetic field. The results presented herein help to narrow down existing theoretical models and stimulate future experimental and theoretical studies.

Acknowledgement The work at the University of Michigan is primarily supported by the National Science Foundation under Award No.DMR-2317618 (thermodynamic measurements and thermoelectric property measurements). The magnetization measurements at the University of Michigan are supported by the Department of Energy under Award No. DE-SC0020184. A portion of this work was performed at the National High Magnetic Field Laboratory (NHMFL), which is supported by National Science Foundation Cooperative Agreement Nos. DMR-1644779 and DMR-2128556 and the Department of Energy (DOE). J.S. acknowledges support from the DOE BES program "Science at 100 T," which permitted the design and construction of much of the specialized equipment used in the high-field studies. The experiment in NHMFL is funded in part by a QuantEmX grant from ICAM and the Gordon and Betty Moore Foundation through Grant No. GBMF5305 to K.-W.C., D. Z., G.Z., A.C., Y.Z., and K.J.. This work at Kyoto University was supported in part by the Japan Society for the Promotion of Science (JSPS) KAKENHI Grant Number 23H00089 and the Japan Science and Technology Agency (JST) CREST Grant Number JPMJCR19T5 awarded to Y. M..

Data availability The data that support the findings of this article are openly available [48].

†K.-W.C. and Y.Z. contributed equally to this work.
*luli@umich.edu

[1] D. Shoenberg, Magnetic Oscillations in Metals, Cambridge Monographs on Physics. Cambridge University Press (1984).

[2] G. Li et al., Two-dimensional Fermi surfaces in Kondo insulator SmB_6. Science, 346, 1208 (2014).

[3] B. S. Tan et al., Unconventional Fermi surface in an insulating state, Science **349**, 287 (2015)

[4] Z. Xiang et al., Quantum oscillations of electrical resistivity in an insulator. Science **362**, 65 (2018).

[5] H. Liu, M. Hartstein, G. J. Wallace, A. J. Davies, M. C. Hatnean, M. D. Johannes, et al. Fermi surfaces in Kondo insulators, Journal of Physics: Condensed Matter **30**, 16LT01 (2018).

[6] Y. Sato et al., Unconventional thermal metallic state of charge neutral fermions in an insulator, Nat. Phys. **15**, 954-959 (2019)

[7] A. Mizzi et al., The reverse quantum limit and its implications for unconventional quantum oscillations in YbB_{12} Nat. Comm. **15**, 1607 (2024).

[8] Z. Xiang et al., Hall Anomaly, Quantum Oscillations and Possible Lifshitz Transitions in Kondo Insulator YbB_{12}: Evidence for Unconventional Charge Transport. Phys. Rev. X **12**, 021050 (2022).

[9] D. Xiao et al., Anomalous quantum oscillations of interacting electron-hole gases in inverted type-II InAs/GaSb quantum wells, Phys. Rev. Lett. **122**, 186802(2019)

[10] Z. Han, T. Li, L. Zhang, G. Sullivan and R.-R. Du, Anomalous conductance oscillations in the hybridization gap of InAs/GaSb quantum wells, Phys. Rev. Lett. **123**, 126803 (2019)

[11] G. Zheng et al., Unconventional Magnetic Oscillations in Kagome Mott Insulators, Proc. Natl. Acad. Sci. U.S.A. 122 (5) e2421390122 (2025)

[12] G. Zheng et al., Thermodynamic evidence of fermionic behavior in the vicinity of one-ninth plateau in a kagome antiferromagnet, Phys. Rev. X, 15(2), 021076 (2025)

[13] Yang, Z., Marcenat, C., Kim, S. et al. Evidence for large thermodynamic signatures of in-gap fermionic quasiparticle states in a Kondo insulator. Nat Commun 15, 7801 (2024).

[14] C. M. Varma, Majoranas in mixed-valence insulators, Phys. Rev. B 102, 155145 (2020)

[15] C. M. Varma, Dark Fermions in Mixed Valence Insulators arXiv:2306.14124 (2023).

[16] D. Chowdhury, I. Sodemann, T. Senthil, Mixed-valence insulators with neutral Fermi surfaces, Nature Commun. 9, 1766 (2018)

[17] P. Rao and I. Sodemann, Cyclotron resonance inside the Mott gap: A fingerprint of emergent neutral fermions, Phys. Rev. B 100, 155150 (2019)

[18] J. T. Heath, K. S. Bedell, Universal signatures of Majorana-like quasiparticles in strongly correlated Landau–Fermi liquids, J. Phys.: Condens. Matter 32 485602 (2020)

[19] O. Erten et al., Skyrme Insulators: Insulators at the Brink of Superconductivity, Phys. Rev. Lett. 119, 057603 (2017)

[20] N. R. Cooper, J. Kelsall, Quantum oscillations in an impurity-band Anderson insulator, SciPost Phys. 15, 118 (2023)

[21] O. Erten, P. Ghaemi, and P. Coleman, Kondo Breakdown and Quantum Oscillations in SmB6, Phys. Rev. Lett. 116, 046403 (2016)

[22] H. Shen and L. Fu, Quantum Oscillation from In-Gap States and a Non-Hermitian Landau Level Problem, Phys. Rev. Lett. 121, 026403 (2018)

[23] N. Harrison, Highly Asymmetric Nodal Semimetal in Bulk SmB6, Phys. Rev. Lett. 121, 026602 (2018)

[24] J. Knolle and N. R. Cooper, Excitons in topological Kondo insulators: Theory of thermodynamic and transport anomalies in SmB6, Phys. Rev. Lett. 118, 096604 (2017)

[25] W. T. Fuhrman and P. Nikolić, Magnetic impurities in

Kondo insulators: An application to samarium hexaboride, Phys. Rev. B 101, 245118 (2020)
[26] Y. Tada, Cyclotron resonance in Kondo insulator, Phys. Rev. Research 2, 023194 (2020)
[27] P. Ram and B. Kumar, Theory of quantum oscillations of magnetization in Kondo insulators, Phys. Rev. B 96, 075115 (2017)
[28] Z. Xiang et al., Unusual high-field metal in a Kondo insulator, Nat. Phys. **17**,788-73 (2021).
[29] A. A. Abrikosov, Fundamentals of the Theory of Metals: Courier Dover Publications, (2017).
[30] H. Liu, Fermi surface in magnetic field-induced metallic YbB_{12}, npj Quantum Materials 7, 12 (2022)
[31] Y. Aoki et al., Thermal properties of metamagnetic transition in heavy fermion systems, J. Magn. Magn. Mater. **177**, 271 (1998).
[32] Z. Shao et al., Acta Phys. Sin. **63**, 240502 (2014).
[33] K. Behnia. Fundamentals of thermoelectricity. OUP Oxford, (2015).
[34] H. Pfau et al., Cascade of Magnetic-Field-Induced Lifshitz Transitions in the Ferromagnetic Kondo Lattice Material $YbNi_4P_2$, Phys. Rev. Lett. **119**, 126402 (2017).
[35] B. McCombe and G. Seidel, Magnetothermal Oscillations and Spin Splitting in Bismuth and Antimony, Phys. Rev. **155**, 633 (1967).
[36] P. F. Sullivan and G. Seidel, Steady-State, ac-Temperature Calorimetry, Phys. Rev. **173**, 679 (1968).
[37] S. C. Riggs et al., Heat capacity through the magnetic-field-induced resistive transition in an underdoped high-temperature superconductor, Nat. Phys. **7**, 332 (2011).
[38] V. Bondarenko et al., First observations of the heat capacity quantum oscillations in the organic superconductor (BEDT-TTF)$_2$Cu(NCS)$_2$, Synth. Met. **120**, 1039 (2001).
[39] K. Sugiyama et al., Field-induced metallic state in YbB_{12} under high magnetic field. J. Phys. Soc. Jpn **57**, 3946–3953 (1988).
[40] S. Tagliati, V. M. Krasnov, and A. Rydh, Differential membrane-based nanocalorimeter for high-resolution measurements of low-temperature specific heat, Rev. Sci. Instrum. 83, 055107 (2012).
[41] K. S. Nemkovski et al., Polarized-Neutron Study of Spin Dynamics in the Kondo Insulator YbB_{12}. Phys. Rev. Lett. **99**, 137204 (2007)
[42] T. T. Terashima et al., Magnetization process of the Kondo insulator YbB_{12} in ultrahigh magnetic fields. J. Phys. Soc. Jpn **86**, 054710 (2017)
[43] Z. Yang et al., Unveiling the double-peak structure of quantum oscillations in the specific heat, Nat. Comm. **14**, 7006 (2023).
[44] See Supplemental Material at [URL will be inserted by publisher], which includes Refs. [8, 28, 29, 40–43, 45–47].
[45] Y. H. Matsuda et al. Suppression off-electron itinerancy in $CeRu_2Si_2$ by a strong magnetic field. Phys. Rev. B **86**, 041109 (2012).
[46] J. Flouquet, et al. Itinerant metamagnetism of $CeRu_2Si_2$: bringing out the dead. Comparison with the new $Sr_3Ru_2O_7$ case. Physica B: Condensed Matter 319.1-4: 251-261 (2002).
[47] J. X. Boucherle, et al. Magnetic form factor in $CeRu_2Si_2$ on crossing its metamagnetic transition. Journal of Physics: Condensed Matter 13.48: 10901 (2001).
[48] K-W. Chen, Y. Zhu, et al., Quantum oscillations in the heat capacity of Kondo insulator YbB12 (2025), https://osf.io/kgxeb/